Turbulence regulation and transport barriers in laboratory plasmas

Kim, E. J.

Original citation:
Kim, EJ 2006, 'Turbulence regulation and transport barriers in laboratory plasmas' Journal of Physics: Conference Series, vol. 44, no. 1, 002, pp. 10-19.
https://dx.doi.org/10.1088/1742-6596/44/1/002

DOI 10.1088/1742-6596/44/1/002
ISSN 1742-6588
ESSN 1742-6596

Publisher: IOP Publishing

Turbulence regulation and transport barriers in laboratory plasmas

Institute of Physics Publishing Journal of Physics: Conference Series **44** (2006) 10–19
doi:10.1088/1742-6596/44/1/002 First International Workshop and Summer School on Plasma Physics (IWSSPP'05)

Turbulence regulation and transport barriers in laboratory plasmas

Eun-jin Kim

Department of Applied Mathematics,University of Sheffield,Sheffield,S3 7RH, UK

E-mail: e.kim@shef.ac.uk

Abstract. We discuss the effect of shearing on transport and the formation of transport barriers. The focus is primarily on laboratory plasmas where the formation of transport barrier (the L–H transition or the formation of internal transport barrier) is thought to originate from turbulence regulation by shearing by (coherent) mean $\mathbf{E} \times \mathbf{B}$ flows and (random) zonal flows. We provide quantitative discussion on the reduction of turbulent transport by these flows and elucidate their roles in the barrier formation.

1. Introduction

Shear flows, which are common features in many physical systems, play an important role in determining turbulent transport. In particular, a shear flow that is stable reduces turbulent transport in the direction orthogonal to the flow (i.e., shear direction) via the so-called enhanced turbulence decorrelation [1, 2]. The basic physics underlying the latter is the distortion and ultimate disruption of a fluid eddy via shearing (when the dissipation becomes sufficiently on small scales) as a shear flow advects different parts of the eddy at different rates. One remarkable consequence of this turbulence regulation via shearing is the formation of transport barrier, which has emerged as one of the crucial mechanisms for controlling mixing and transport in a variety of systems. For instance, equatorial wind in the atmosphere has been known to inhibit the latitudinal mixing [3] while the formation of transport barrier by a shear layer in the ocean was recently recognized [4]. In this paper, we discuss quantitatively how shearing leads to transport reduction and thus barrier formation. The application is primarily to laboratory plasmas for which a shear flow is stable against Kelvin–Helmholtz instability [5] because of magnetic shear [6], and thus plays a crucial role in regulating turbulence, reducing heat and/or particle losses to a container wall via turbulent transport. This is a crucial feature for a future economical reactor as its main goal is to extract as much nuclear fusion energy as possible, by confining hot plasmas in the core for a sufficiently long time [7].

In fusion devices, the confinement of particles and heat degrades as the input power is ramped up [7]. This is simply because the input power is stored as free energy in background (e.g., density and temperature) profiles, which is then released by various microinstabilities. These microinstabilities cause anomalous transport of heat and particles toward a container wall, thereby degrading confinement. However, as input power is further increased beyond a critical value, plasmas undergo a bifurcation by the formation of transport barriers at the plasma edge, whereby organizing themselves into a high confinement state. At this transition, the confinement time is roughly doubled. This is the so-called L–H transition (namely, the

transition from low to high confinement modes). This transition seems to be universal as it has been reproduced in a variety of fusion devises since its first discovery in ASDEX [8]. It is now understood that this transition is caused by the formation of a transport barrier at the plasma edge via enhanced shear decorrelation. Thus, a simple criterion for the transition is crudely given in terms of the shearing rate (Ω), and requires that Ω should exceed the decorrelation rate of the underlying turbulence. Although this criterion becomes more complex in tokamaks [9] due to other physical effects (such as magnetic shear, etc), it has nevertheless been widely used as a rough estimate on the critical shear strength necessary for the L–H transition. Later, the barrier formation towards plasma core (the so-called internal transport barrier) (see, e.g., [10]) has also been observed, and the shear decorrelation is also thought to be one of the main causes leading to this phenomenon [1]. Similar transport reduction and barrier formation via shearing also take place in other systems, including the atmosphere and ocean [3, 4].

The remainder of the paper is organized as follows. In Sec. 2, we discuss two types of shear flows – mean and zonal flows – and their roles in the L–H transition. In Sec. 3, a simple L–H transition model is discussed which can identify the important roles that mean and zonal flows play in the transition. In Sec. 4, turbulence regulation by mean and zonal flows is compared, and the detailed study of the reduction of turbulent transport by these flows is presented for the passive scalar field model. The reduction in particle transport is addressed in a more realistic dynamical model in Sec 5. Section 6 contains conclusions.

2. Shear flows in fusion plasmas

A shear flow, which is important in regulating turbulent transport in fusion plasmas, is a mean $\mathbf{E}\times\mathbf{B}$ flow (i.e., $\langle\mathbf{V}_{\rm E}\rangle = c\mathbf{E}\times\mathbf{B}/B^2$). This is excited by mean pressure gradient, mean poloidal and toroidal flows $\langle\mathbf{V}\rangle$, and external momentum source as well as Reynolds stress through the radial force balance for ions with charge q as:

$$0 = \langle -\nabla p + q\mathbf{E} + \frac{q}{c}\mathbf{V}\times\mathbf{B} + \mathbf{\Gamma}\rangle\,. \tag{1}$$

Here, the angular brackets denote the average over small-scales, and $\mathbf{\Gamma}$ includes the nonlinear Reynolds stress drive and the external torque such as neutral beam injection. As its name implies, a mean shear flow varies on long time scale with smooth spatial structure. Thus, the shearing by mean flows is coherent. Indeed, the turbulence regulation, causing the L–H transition, was originally thought to be due to this mean flow $\langle\mathbf{V}_{\rm E}\rangle$, and numerous works were devoted to L–H transition modelling by using mean flow as turbulence regulating mechanism.

However, various recent numerical studies suggested that self-generated shear flows (the so-called zonal flows) also play a crucial role in regulating turbulence. For instance, [11] demonstrated the significant increase in turbulence level when self-generated zonal flows are artificially suppressed. These are radially localized, poloidal $\mathbf{E}\times\mathbf{B}$ flows due to radial electric field $\mathbf{E}$, nonlinearly generated from (drift-wave) turbulence (i.e., $\mathbf{V}_{\rm E} = c\mathbf{E}\times\mathbf{B}/B^2$). Unlike mean flows, zonal flows are solely driven nonlinearly from underlying turbulence by modulational instability (similar to inverse cascade in 2D hydrodynamic turbulence) [12]. Thus, they are very likely to be structured and possibly even random in both space and time, with finite correlation time $\tau_{\rm ZF}$. Consequently, the efficiency of zonal flow shearing depends on $\tau_{\rm ZF}$, compared to other characteristic time scales, as discussed in detail in Sec. 4. Roughly, its shearing rate, due to (spatial or temporal) stochasticity, is given by its RMS value $\Omega_{\rm rms} = \sqrt{\langle(\partial_r V_{\rm E})^2\rangle^{1/2}}$. Furthermore, zonal flows and turbulence constitute an interesting self-regulating system, like a predator-prey model, via the generation of zonal flows by turbulence and turbulence regulation by zonal flows. This self-regulation can result in the time-transient behavior in a system [13].

In L mode, the pressure gradient is rather weak to drive a strong mean flow while Reynolds stress drive for zonal flows, with finer spatial structure, is likely to be much stronger than that

for a mean $\mathbf{E}\times\mathbf{B}$ flow. Therefore, in the absence of mean poloidal and toroidal flows and external momentum source, (RMS) shearing rate of zonal flows (i.e., $\Omega_{\rm rms}=\sqrt{(\partial_r V_{\rm E})^2}$), with large spatial gradient in a flow, may dominate over that by mean flow (i.e., $|\partial_r\langle V_{\rm E}\rangle|$) before the transition, with the possibility of zonal flows triggering the L–H transition [14, 15]. As plasmas undergo the transition, the pressure profile steenpens, thereby driving a strong mean shear flow. Therefore, shearing by mean flow becomes important after the transition, and maintains the plasma in H-mode [15]. This will be discussed further in Sec. 3. Note that zonal flows in laboratory plasmas have much in common with zonal winds in major planets and in the earth atmosphere in their origins and effects on transport.

3. The L–H transition

As indicated in Sec. 2, both mean $\mathbf{E}\times\mathbf{B}$ flow and zonal flows are responsible for the L–H transition in fusion plasmas. As they have different characters and origins (see Sec. 2), it is important to disentangle their roles in the formation of transport barriers and thus in the L–H transition. In this section, we discuss the implications of the difference in their origins for the L–H transition through the qualitative study of a specific model for the transition.

At the simplest level, we can examine the roles of mean and zonal flows in the transition, by assuming that the reduction in turbulence amplitude (rather than the turbulent transport) by both mean and zonal flows is responsible for the transition, and that the mean flow is solely driven by ion pressure gradient [15] (by ignoring mean poloidal and toroidal flows and external momentum source). Then, the essential physics of the transition can be captured by the following 0-dimensional (0D) envelop equations for turbulence amplitude $\tilde{E}$, zonal flow shear $V_{\rm ZF}\propto\partial_r\tilde{V}_{\rm E}$, mean flow shear $V\propto\partial_r\langle V_{\rm E}\rangle$, and the gradient of mean ion pressure $\mathcal{N}$ as:

$$\partial_t\tilde{E} = \tilde{E}\mathcal{N}-a_1\tilde{E}^2-a_2V^2\tilde{E}-a_3V_{\rm ZF}^2\tilde{E}\,, \tag{2}$$

$$\partial_t V_{\rm ZF} = b_1\frac{\tilde{E}V_{\rm ZF}}{1+b_2V^2}-b_3V_{\rm ZF}\,, \tag{3}$$

$$\partial_t\mathcal{N} = -c_1\tilde{E}\mathcal{N}-c_2\mathcal{N}+Q\,, \tag{4}$$

$$V = d\mathcal{N}^2\,. \tag{5}$$

Here, a_i, b_i, c_i and d are model-dependent constants. The exact form of these constants is not pertinent to the qualitative understanding of the transition, so will not be discussed here.

The physical meaning of each term in Eqs. (2)–(5) is as follows. First, Eq. (2) describes the evolution of turbulence: the first term on the right hand side represents turbulence generation by pressure gradient via linear instability, the second nonlinear saturation of turbulence, and the third and last terms shear suppression of turbulence by mean $\mathbf{E}\times\mathbf{B}$ flows and zonal flows, respectively. The evolution of the zonal flow shear $V_{\rm ZF}$ in Eq. (3) is governed by its generation by Reynolds stress and zonal flow damping as represented by the first and second terms, respectively, on the right hand side. The growth of zonal flows is inhibited by a mean shear flow since the mean flow weakens the response of turbulence (drift wave) spectrum to a seed zonal flow via the enhanced decorrelation of drift wave propagation by a mean shear flow [16]. This effect is modelled by a term $1/(1+b_2V^2)$. Eq. (4) represents the evolution of pressure gradient as a result of the turbulent diffusion of the pressure profile by turbulence ($c_1\tilde{E}$), neoclassical transport (c_2), and input power Q, respectively. Eq. (5) is the gradient of ion momentum balance relation with a constant ion temperature profile in the absence of mean toroidal and poloidal mean flows and external source. That is, the mean flow shear shear V is solely generated by mean pressure gradient $\mathcal{N}$ (or mean density gradient).

The input power Q is the control parameter of Eqs. (2)–(5). Let us examine how the system evolves as this control parameter is increased from below. As Q increases, the mean pressure gradient becomes steeper and excites turbulence. When the turbulence drive becomes sufficiently

strong to overcome flow damping, it generates zonal flows by Reynolds stress. Turbulence and zonal flows then form a self-regulating system as the shearing by zonal flows damps the turbulence. A signature of this self-regulation is manifested in time transient (oscillatory or bursty) behavior of the system [13, 17, 18, 13, 19]. For a sufficiently high Q, this self-regulation turns off the turbulence, and subsequently zonal flows are depleted by a mean shearing, with the system evolving into a quiescent H mode

$$\tilde{E} = V_{\rm ZF} = 0\,, \mathcal{N} = \frac{Q}{c_2}\,. \tag{6}$$

Here, the slope of the profile is determined by neoclassical transport c_2. This quiescent H mode will eventually terminate upon the further increase of gradients when MHD instability sets in. This regime, however, shall not be discussed in this paper.

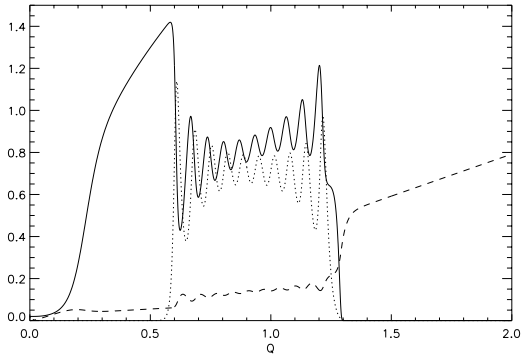

Figure 1. Evolution of $\tilde{E}$ (solid line), $V_{\rm ZF}$ (dotted line), and $\mathcal{N}/5$ (dashed line) as a function of input power $Q = 0.01t$. Parameter values are $a_1 = 0.2$, $a_2 = a_3 = 0.7$, $b_1 = 1.5$, $b_2 = b_3 = 1$, $c_1 = 1$, $c_2 = 0.5$, and $d = 1$.

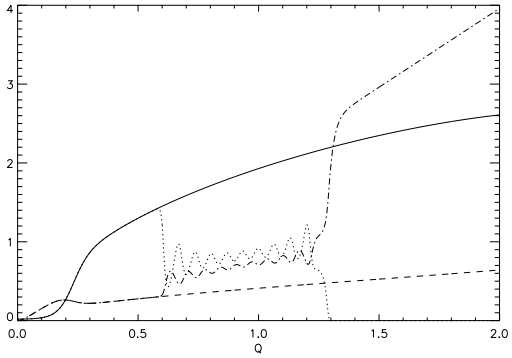

Figure 2. Evolution of $\tilde{E}$ (solid line) and $\mathcal{N}$ (dashed line) with $V_{\rm ZF} = 0$. The parameter values are the same as in figure 1. $\tilde{E}$ (dotted line) and $\mathcal{N}$ (dotted–dashed line) in figure 1 are superimposed.

The evolution into a quiescent H mode is quantitatively shown in figure 1, by numerically solving Eqs. (2)–(5) with $Q = 1.0 \times 10^{-2}t$ (t is time) and constant values for parameters a_i, b_i, c_i, and d. The solid, dotted, and dashes lines represent the evolution of $\tilde{E}$, $V_{\rm ZF}$, and $\mathcal{N}/5$, respectively. There are three distinct stages; The early stage is characterized by growing turbulence (by linear instability from increasing $\mathcal{N}$), followed by rapidly growing self-generated zonal flows. As the shearing by zonal flows becomes sufficient to damp turbulence, the system self-regulates, entering into a transition regime, where zonal flows and turbulence compete and exhibit oscillatory behavior: $\tilde{E}$ and $V_{\rm ZF}$ grow as they draw energy from $\mathcal{N}$ and $\tilde{E}$, respectively, while $\tilde{E}$ and $\mathcal{N}$ damp on account of growing $V_{\rm ZF}$ and $\tilde{E}$, respectively. The gradual increase in $\tilde{E}$ in figure 1, in addition to oscillation, is due to the reduction in the zonal flow growth by the mean shear flow, which promotes the growth of turbulence. A slight decrease in the amplitude of oscillation is due to nonlinear damping of drift waves ($a_2\tilde{E}^2$). The behavior of this envelope is given by a stationary solution $\tilde{E} = b_1(1 + b_2V^2)/b_3$ (see Eq. (3)), which increases as the profile steepens ($V = d\mathcal{N}^2$). The final stage of the evolution (i.e., a quiescent H mode) is marked by the complete damping of turbulence and zonal flows due to strong mean flow shearing for sufficiently large Q. At this stage, the profile steepens linearly with Q, consistent with Eq. (6).

Since zonal flows regulate turbulence before the transition to a quiescent H mode, they trigger the transition by lowering the power threshold, relative to the case without zonal flows. To see this important effect, we plot $\tilde{E}$ (solid) and $\mathcal{N}$ (dashed line) in figure 2 for the same parameters

values as in figure 1, but with $V_{\rm ZF} = 0$, where it can clearly be seen that the turbulence amplitude is too large to reach a quiescent H mode for the values Q up to 2. For comparison, the Q dependence of $\tilde{E}$ and $\mathcal{N}$ in figure 1 are superimposed by dotted and dotted–dashed lines, respectively, in figure 2.

A detailed test of the role of zonal flows in L–H transition and identification of the origin of the oscillatory behavior remains as a challenge to experimentalists. First of all, a careful control over the input power ramping is necessary, since the duration of the transition regime sensitively depends on the rate of input power ramping – too rapid ramping shrinks this regime to an arbitrary short time interval, smaller than that of the experimental time resolution. Secondly, the distinction between mean poloidal flows and zonal flows should be made experimentally. A recent experiment on DIII-D [20] successfully resolved a time transient regime (IM mode) by slowly increasing the input power. However, the time transient behavior was interpreted to originate from a self-generated poloidal flow, without a clear identification of the latter. In the model considered in this section, the zonal flow was the main source of a poloidal flow, in view of the weak Reynolds stress drive for mean poloidal flow.

4. Turbulent reduction in passive scalar model

In this section, we discuss quantitatively how both mean and zonal flows lead to enhanced decorrelation of the two nearby particles and turbulence regulation in the passive scalar field model in 2D. Passive scalar fields n are assumed to be advected by random turbulent flow $\mathbf{v}$ with $\langle \mathbf{v} \rangle = 0$ and by a mean or zonal flow $\mathbf{U} = U(x,t)\hat{y}$ ($\langle \mathbf{U} \rangle = \mathbf{U}$). Here, the spatial profile of $U(x,t)$ is taken to be linear in x (i.e., $U(x,t) = -x\Omega(t)$); angular brackets denote ensemble average over the statistics of turbulent flow $\mathbf{v}$; x and y denote local radial and poloidal directions, respectively. Since we are primarily interested in the scalings of turbulent transport near the L–H transition where shearing rate can exceed the nonlinear decorrelation rate of turbulence (i.e., the strong shear limit), we can assume the turbulence to be weak and use a quasi-linear analysis. By assuming that fluctuating fields vary on scales much smaller than mean fields, the evolution of fluctuating component n' can be written as

$$[\partial_t + U(x,t)\partial_y]n' = -v_x \partial_x n_0 + D(\partial_{xx} + \partial_{yy})n' \,. \tag{7}$$

Here, n' and $n_0 = \langle n \rangle$ are fluctuating and mean parts of n ($n = n_0 + n'$), and D is the effective diffusivity, including nonlinear interaction. The advection by a linear shear flow $U(x,t) = -x\Omega(t)$ results in the distortion of an eddy (i.e., wind-up), and its effect can be non-perturbatively captured by employing time-dependent wavenumber $k_x(t)$ with the following transformation for n:

$$n'(\mathbf{x},t) = \tilde{n}(\mathbf{k},t) \exp\left\{ i(k_x(t)x + k_y y) \right\} , \tag{8}$$

and similarly for v_x, with k_x satisfying an eikonal equation

$$\partial_t k_x(t) = k_y \Omega(t) \,. \tag{9}$$

The solution to Eq. (7) can thus be expressed as:

$$\tilde{n}(\mathbf{k},t) \;\; = -\partial_x n_0 \;\; \int_{-\infty}^{t} dt_1 d^2k_1 \hat{g}(\mathbf{k},t;\mathbf{k}_1,t_1) e^{-DQ(t,t_1)} \tilde{v}_x(\mathbf{k}_1,t_1) \,. \tag{10}$$

Here, $Q(t,t_1) = \int_{t_1}^{t} dt' [k_x^2(t') + k_y^2]$, and $\hat{g}$ is the Green's function given by

$$\hat{g}(\mathbf{k},t;k_1,t_1) = \delta(k_y - k_{1y}) \delta \left[k_x - k_{1x} - k_{1y} \int_{t_1}^{t} dt' \Omega(t') \right] . \tag{11}$$

It is important to note that the overall effect of enhanced dissipation by shearing is embedded as the time integral of k^2 in DQ in the argument of exponential in Eq. (10).

4.1. Comparison between coherent and random shearing

The characteristic shearing time scales due to mean and zonal flows are $\tau_\Omega = \Omega^{-1}$ and $\Omega_{\rm rms}^{-1}$, respectively. We now examine how the shearing by both mean and zonal flows speeds up the decorrelation of the two nearby particles in the strong shear limit where the shearing takes place on time scale shorter than turbulent diffusive time scale $\tau_\eta = 1/Dk^2$, i.e., when $\tau_\Omega \ll \tau_\eta$. Here, D is the effective diffusivity including the effect of nonlinear mixing; $1/k$ is the characteristic scale of turbulence. Note that $\tau_\eta^{-1} = Dk^2$ is the decorrelation rate in the absence of shearing.

In the case of coherent shearing, $\Omega(t) = \Omega$ is constant, with k_x linearly increasing in time t (see Eq. (9)), i.e., $k_x(t) \propto k_y \Omega t$. Thus, the overall effect of dissipation DQ in Eq. (10) becomes

$$DQ(t, t_1) \propto Dk_y^2(t + \Omega^2 t^3) \sim Dk_y^2 \Omega^2 t^3 = t^3/(\tau_\eta \tau_\Omega^2) \tag{12}$$

in the long time limit, leading to the following characteristic decorrelation time:

$$\tau_\Delta = (\tau_\eta \tau_\Omega^2)^{1/3}\,. \tag{13}$$

Thus, a strong (steady) shear (i.e., $\tau_\Omega/\tau_\eta \to 0$) enhances the decorrelation rate of two nearby fluid elements to $\tau_\Delta^{-1} = (Dk^2\Omega^2)^{1/3} = (\tau_\eta \tau_\Omega^2)^{-1/3} > \tau_\eta^{-1}$ above the value $\tau_\eta^{-1} = Dk^2$ determined by turbulent scattering alone [21].

Random shearing by zonal flows with finite correlation time $\tau_{\rm ZF} < \tau_\eta$ also enhances the decorrelation rate, but it is less efficient as compared to coherent shearing since shearing changes its direction in time. For instance, over a time scale much longer than the diffusive time scale (i.e. $t \gg \tau_\eta \gg \tau_{\rm ZF}$), zonal flows can be assumed to have a short correlation time. Thus, in the long time limit, the evolution of $k_x(t)$ can be considered as a random Markovian process with a short memory, with $[k_x(t) - k_x(0)]^2 = k_y^2 \int^t dt_1 \int^t dt_2 \Omega(t_1)\Omega(t_2) \sim k_y^2 \Omega_{\rm rms}^2 \tau_{\rm ZF} t = k_y^2 \Omega_{\rm eff} t$. Here, $\Omega_{\rm eff} = \tau_{\rm ZF}\Omega_{\rm rms}^2$ is the effective shearing rate of zonal flows. Thus, the overall dissipation becomes

$$DQ(t, t_1) \sim D \int^t dt' k_x^2(t') \propto \Omega_{\rm eff} t^2/\tau_\eta, \tag{14}$$

which increases only quadratically with time (cf. Eq. (12)). Eq. (14) gives us the effective decorrelation time $\tau_{\rm D}$ in the case of random shearing as

$$\tau_{\rm D} = (\tau_\eta/\Omega_{\rm eff})^{1/2}. \tag{15}$$

$\tau_{\rm D}$ in Eq. (15) is still smaller than τ_η in the strong shear limit $\tau_\Omega/\tau_\eta \to 0$. However, $\tau_{\rm D}$ is larger than τ_Δ in the case of coherent shearing for $\Omega = \Omega_{\rm rms}$. This is because a longer decorrelation time is induced by finite $\tau_{\rm ZF}$, with less efficient shearing by zonal flows.

In contrast, when $\tau_{\rm ZF}$ becomes large enough to satisfy $\tau_{\rm ZF} \gg (\tau_{\rm D}, \tau_\eta)$, shearing by zonal flows can be considered to be coherent, with the results similar to those for a steady shear flow, with Ω replaced by $\Omega_{\rm rms}$ [22]. Furthermore, it turns out that in the case of a steady zonal flow with complex spatial dependence, the same scalings of flux and amplitude of scalar fields with $\langle U'^2\rangle^{1/2}$ are obtained as those with Ω in the case of a steady linear shear flow [22].

4.2. Turbulence reduction by mean and zonal flows

Let us assume that the random turbulent flow has characteristic correlation time $\tau_{\rm c}$ and is statistically homogeneous and steady with the following correlation function:

$$\langle \tilde{v}_x(\mathbf{k}_1, t_1)\tilde{v}_x(\mathbf{k}_2, t_2)\rangle = (2\pi)^2 \delta(\mathbf{k}_1 + \mathbf{k}_2)\phi(\mathbf{k}_2, t_2 - t_1)\,, \tag{16}$$

where ϕ is assumed to be dominated by modes with $k_x \ll k_y$.

Table 1. Scalings in the case of coherent shearing by mean flows in passive scalar field model.

	$\tau_c < \tau_\Omega$	$\tau_\Omega < \tau_c$
$\langle n' v_x \rangle$	Ω^0	Ω^{-1}
$\langle n'^2 \rangle$	$\tau_\Delta \propto \Omega^{-1}$	$\tau_\Delta \Omega^{-1} \propto \Omega^{-5/3} D^{-1/3}$

In the case of coherent shearing by mean shear flows, or zonal flows with long correlation time ($\tau_{ZF} > \tau_\eta > \tau_D$), physically two interesting cases are when (i) $\tau_c \ll \tau_\Omega \ll \tau_\eta$ and (ii) $\tau_\Omega \ll \tau_c \ll \tau_\eta$. Case (i) corresponds to delta-correlated turbulent flow, where the irreversibility mainly arises from the randomness of the flow while in case (ii), the mean flow–wave resonance is the main source of irreversibility. Stronger reduction in the flux and turbulence amplitude is obtained in case (ii) since shearing is more efficient in distorting turbulent eddy when $\tau_c > \tau_\Omega$. This is shown in table 1, which contains the summary of scalings. Note that the flux is reduced by shearing only in case (ii), but rather weakly with the scaling Ω^{-1}. This reduction is too weak to explain experimental results of a significant reduction in the transport of particle or heat, with scaling $\propto \Omega^{-\alpha}$ where $1.6 \lesssim \alpha \lesssim 4.8$ [23, 24]. Furthermore, these results with different scalings, depending on the ordering among different time scales, suggest that there is no universal scalings of flux and turbulence amplitude with Ω. That is, the scalings of turbulence intensity and transport depend on the property of the random turbulent flows, i.e., the magnitude of their correlation time (τ_c) relative to shearing time ($\tau_\Omega = \Omega^{-1}$).

Table 2. Scalings in the case of random shearing by zonal flows in passive scalar field model.

	$\tau_c < \tau_\Omega$	$\tau_\Omega < \tau_c$
$\langle\langle n' v_x \rangle\rangle$	Ω^0_{rms}	Ω^{-1}_{rms}
$\langle\langle n'^2 \rangle\rangle$	$\tau_D \propto \Omega^{-1}_{rms}$	$\tau_D \Omega^{-1}_{rms} \propto \Omega^{-2}_{rms} D^{-1/2}$

In the case of random shearing by zonal flows with short correlation time ($\tau_{ZF} < \tau_D < \tau_\eta$), the flux and turbulence amplitude should be averaged over zonal flows, in addition to that of the turbulent flow $\mathbf{v}$. Thus, we use double angular brackets $\langle\langle\rangle\rangle$ to denote the average over the two. One interesting consequence of random shearing with no net mean shear ($\langle\langle\Omega\rangle\rangle = 0$) is the replacement of resonance between the flow and turbulence (where a local Doppler shifted frequency vanishes) by a smooth, probabilistic interaction kernel.

The results are provided in table 2. Stronger reduction is, again, obtained when $\tau_\Omega < \tau_c$. In the case of short τ_c with $\tau_c < \tau_\Omega$, the scalings of the flux and turbulence amplitude with Ω_{rms} are similar to those with Ω for coherent shearing, given in table 1. However, when $\tau_c > \tau_\Omega$, turbulence amplitude has a stronger dependence on Ω_{rms} as Ω^{-2}_{rms} than $\Omega^{-5/3}$ for coherent shearing. Despite this stronger dependence, the turbulence amplitude in the case of random shearing $\langle n'^2 \rangle \propto \tau_D/\Omega_{rms}$ is still larger than that $\langle n'^2 \rangle \propto \tau_\Delta/\Omega$ in the case of coherent shearing in table 1 when $\Omega = \Omega_{rms}$. This is just because zonal flows with finite τ_{ZF} lead to less efficient shearing with a longer effective decorrelation time of fluid elements $\tau_D > \tau_\Delta$. For instance, the amplitude increases as τ_{ZF} becomes small (since $\Omega_{eff} \to 0$ and $\tau_D \to \infty$). The upper limit on the amplitude is, however, given by $\tau_D = (D k_y^2 \Omega^2_{rms})^{-1}$. As τ_{ZF} exceeds τ_D, zonal flows can be considered to be steady in time, thus recovering previous result for a steady shear flow.

5. Dynamical Models

It is not surprising that the passive scalar field model does not explain the strong reduction in the heat or particle transport that was experimentally observed [23, 24]. The fact is that in this simple-minded model, the properties of the turbulent flow, such as τ_c in relative to τ_Ω, cannot self-consistently be determined. Furthermore, the amplitude of the velocity of turbulent flow is also fixed arbitrarily in that model. That is, the property of the flow is one of the missing ingredients in that model, which can, however, be critical to determining transport level in realistic experimental situation.

To overcome this limitation, the passive scalar field model should be extended to a dynamical one within which the property of the turbulent flow is not arbitrarily prescribed, but is determined self-consistently. As an example, we consider an interchange turbulence model (which is similar to the classical Rayleigh–Bénard convection problem) and examine how the transport of particles is affected by both mean [25] and random shearing. The analysis is limited to the strong shear case where the shearing rate exceeds the nonlinear decorrelation rate of turbulence (i.e., $\tau_\Omega \ll \tau_\eta$).

For simplicity, we assume cold ions and consider the quasi-linear evolution of flute-like perturbations of particle density n and vorticity $\omega = \nabla\times\mathbf{v}$ in a 2D plane, which are subject to a given (poloidal) linear shear flow $U(x,t)\hat{y}$ ($U = -x\Omega(t)$) and effective gravity $\mathbf{g} = g\hat{x}$ (due to magnetic curvature, etc):

$$\partial_t n' + U\partial_y n' = -v_x\partial_x n_0 + D\nabla^2 n' + f\,, \tag{17}$$

$$\partial_t \omega + U\partial_y \omega = -g\partial_y n'/n_0 + \nu\nabla^2\omega\,. \tag{18}$$

Here, $\mathbf{u} = \mathbf{v} + U(x,t)\hat{y}$ is the total velocity with $\mathbf{v} = -(c/B)\nabla\phi\times\hat{z}$, and $n = n_0(x) + n'$ is the total density where $n_0(x) = \langle n\rangle$ are n' are the mean background density and fluctuation; x and y represent the local radial (x) and poloidal (y) directions, perpendicular to a magnetic field $\mathbf{B} = B\hat{z}$; D and ν capture coherent nonlinear interaction as well as molecular dissipation while f represents a noise due to incoherent nonlinear interaction and external particle source. Within this model, density is simply advected by a turbulent flow ($\mathbf{v}$) and a given shear flow $U(x,t)\hat{y}$, similar to passive scalar field, while the flow ($\mathbf{v}$) is dynamically determined.

For simplicity, we assume $D = \nu$, treat the source of free energy $v_x\partial_x n_0$ in Eq. (17) as a part of the noise f and assume that the statistics of the noise f is homogeneous in space and steady in time with a short correlation time $\tau_f < (\tau_\Omega, \tau_{ZF})$:

$$\langle \tilde{f}(\mathbf{k}_1,t_1)\tilde{f}(\mathbf{k}_2,t_2)\rangle = \tau_f(2\pi)^2\delta(\mathbf{k}_1+\mathbf{k}_2)\psi(\mathbf{k}_2)\delta(t_2-t_1)\,. \tag{19}$$

The scalings of correlation functions for both coherent ($\tau_D \ll \tau_{ZF}$) and random shearing ($\tau_D \gg \tau_{ZF}$) by mean and zonal flows are summarized in the second and third columns in table 3, respectively.

Table 3. Scalings in dynamical model.

	$\tau_D \ll \tau_{ZF}$	$\tau_D \gg \tau_{ZF}$
$\langle\langle n'v_x\rangle\rangle$	$\Omega^{-2}\ln(\tau_\Delta\Omega)$	$\tau_D\Omega_{\rm eff}^{-1} \propto \Omega_{\rm rms}^{-3}$
$\langle\langle n'^2\rangle\rangle$	$\tau_\Delta \propto \Omega^{-2/3}$	$\tau_D \propto \Omega_{\rm rms}^{-1}$
$\langle\langle v_x^2\rangle\rangle$	Ω^{-3}	$\tau_D\Omega_{\rm eff}^{-2} \propto \Omega_{\rm rms}^{-5}$
$\langle\langle v_x v_y\rangle\rangle$	$-\Omega^{-3}\ln(\Omega\tau_\eta)$	

In contrast to passive scalar field model where the amplitude of turbulent flow ($\langle v_x^2 \rangle$) is arbitrarily fixed, the latter undergoes severe reduction in both cases, as can be seen in table 3. This severe reduction in velocity amplitude of the turbulent flow is responsible for significant reduction in the particle transport. In particular, in the case of random shearing, the reduction in density flux and the amplitude of velocity is quite strong with the scaling $\Omega_{\rm eff}^{-3/2} \propto \Omega_{\rm rms}^{-3}$ and $\Omega_{\rm eff}^{-5/2} \propto \Omega_{\rm rms}^{-5}$, respectively. However, it is important to realize that turbulence reduction by random shearing is still less severe as compared to coherent shearing for $\Omega_{\rm rms} = \Omega$ since $\tau_{\rm D} > \tau_\Delta$ and $\tau_{\rm D} > \Omega_{\rm eff}^{-1}$. Interestingly, in the case of coherent shearing, a mean flow is generated through Reynolds stress with negative turbulent viscosity $\nu_T \propto -\Omega^{-4} \ln(\Omega\tau_\eta)$ while this Reynolds stress driving itself is reduced by shear as its amplitude becomes large, manifesting self-regulation.

The results shown in table 3 are valid in the limit of short noise correlation time ($\tau_{\rm f} < (\tau_\Omega, \tau_{\rm ZF})$). As $\tau_{\rm f}$ becomes larger than τ_Ω, shearing acts more efficiently due to the coherence of shearing, and thus stronger reduction in the flux and amplitude of turbulence is expected (see, for example, [25]).

6. Conclusions

We have discussed the effect of shearing by both mean and zonal flows on transport and the formation of transport barriers in laboratory plasmas. In particular, we have shown:

(i) Zonal flows trigger L–H transition while mean flows maintain H-mode after the transition.

(ii) Coherent and random shearing by mean and zonal flows lead to short effective decorrelation time $\tau_\Delta = (\tau_\eta \tau_\Omega^2)^{1/3}$ ($< \tau_\eta$) and $\tau_{\rm D} = (\tau_\eta/\Omega_{\rm eff})^{1/2}$ ($< \tau_\eta$) of the two nearby particles, respectively. Here, $\tau_\eta = 1/Dk^2$, $\Omega_{\rm eff} = \tau_{\rm ZF}\Omega_{\rm rms}^2$ and $\tau_\Omega = \Omega^{-1}$ and $\Omega_{\rm rms}^{-1}$ in the case of shearing by mean and zonal flows, respectively. However, random shearing is less efficient with longer decorrelation time $\tau_{\rm D} > \tau_\Delta$ for $\Omega = \Omega_{\rm rms}$.

(iii) Reduction in the flux and turbulence amplitude depends on the model – stronger reduction is obtained in interchange turbulence due to the suppression of velocity amplitude.

(iv) Effect of random shearing of zonal flows on transport and fluctuation levels depends on correlation time $\tau_{\rm ZF}$. While random shearing can lead to significant reduction in interchange turbulence, turbulence amplitude and transport are larger as compared to coherent shearing due to finite correlation time $\tau_{\rm ZF}$.

The transport barrier also takes place in a variety of other systems, and this paper will serve as a guide for understanding the dynamics of those systems.

6.1. Acknowledgments

The author thanks P.H. Diamond and T.S. Hahm for useful discussions.

References

[1] Burrell K H 1997 *Phys. Plasmas* **4** 1499
[2] Kim E and Dubrulle B 2001 *Phys. Plasmas* **8** 813
[3] McIntyre M E 1989 *J. Atmospheric and Terrestrial Phys.* **51** 29
[4] Hunt J C R and Durbin P A 1999 *Fluid Dynamics Research* **23** 375
[5] Drazin P G and Reid W H 1997 *Hydrodynamic Stability* (Cambridge Univ. Press: Cambridge)
[6] Scott B D, Terry P W and Diamond P H 1988 *Phys. Fluids* **31** 1481
[7] Kadomtsev B B 1992 *Tokamak Plasma: A Complex Physical System* (Institute of Phys. Publishing: Bristol and Philadelphia)
[8] Wagner F *et al* 1982 *Phys. Rev. Lett.* **49** 1408
[9] Hahm T S and Burrell K H 1995 *Phys. Plasmas* **2** 1648
[10] Hahm T S 2002 *Plasma Phys. Control. Fusion* **44** A87
[11] Lin Z, Hahm T S, Lee W W, Tang W M and Diamond P H 1999 *Phys. Rev. Lett.* **83** 3645

[12] Diamond P H *et al* 1998 *Plasma Phys. and Controlled Nuclear Fusion Research* (IAEA, Vienna) IAEA-CN-69/TH3/1
[13] Malkov M, Diamond P H and Rosenbluth M N 2001 *Phys. Plasmas* **8** 5073
[14] Moyer R, Tynan G R, Holland C and Burin M J 2001 *Phys. Rev. Lett.* **87** 135001
[15] Kim E and Diamond P H 2003 *Phys. Rev. Lett.* **90** 185006
[16] Kim E and Diamond P H 2003 *Phys. Plasmas* **10** 1698
[17] Jakubowski M, Fonck R J and McKee G R 2002 *Phys. Rev. Lett.* **89** 265003
[18] Shats M G and Solomon W M 2002 *Phys. Rev. Lett.* **88** 045001
[19] Mazzucato E *et al* 1996 *Phys. Rev. Lett.* **77** 3145
[20] Colchin R J *et al* 2002 *Phys. Rev. Lett.* **88** 255002
[21] Biglari H, Diamond P H and Terry P W 1990 *Phys. Fluids B* **2** 1
[22] Kim E and Diamond P H 2004 *Phys. Plasmas* **11** L77
[23] Weynants R R, Jachmich S and Van Oost G 1998 *Plasma Phys. Control. Fusion* **40** 635
[24] Boedo J *et al* 2000 *Phys. Rev. Lett.* **84** 2630
[25] Kim E, Diamond P H and Hahm T S 2004 *Phys. Plasmas* **11** 4554